Journal of Alloys and Compounds 695 (2017) 2965–2968

Contents lists available at ScienceDirect

Journal of Alloys and Compounds

journal homepage: http://www.elsevier.com/locate/jalcom

A facile in-situ growth of large area flexible α-MoO_3 microsheets aligned arrays for temperature sensor

Hong Pan, Long Jin, Hai Su, Binbin Zhang, Lei Zhang, Haitao Zhang, Weiqing Yang*

Key Laboratory of Advanced Technologies of Materials (Ministry of Education), School of Materials Science and Engineering, Southwest Jiaotong University, Chengdu 610031, China

ARTICLE INFO

Article history:
Received 7 July 2016
Received in revised form
22 November 2016
Accepted 25 November 2016
Available online 26 November 2016

Keywords:
Oxidation
MoO_3
Microstructure
Semiconductors

ABSTRACT

We reported a facile, environmentally friendly, in-situ growth and economic thermal oxidization method for growing large area, flexible and aligned α-MoO_3 microsheets arrays (MMAs) on Mo foil. The surface morphology, and cross-sectional images show that the size of rectangle and height of α-MoO_3 microsheets arrays increase with increasing oxidization temperature, and these arrays are strongly adhering to Mo substrate. The aligned α-MoO_3 microsheets arrays have a preferential (100) orientation of the crystallites. Additionally, this kind of MMAs demonstrates the excellent flexibility. Based on it, a simple temperature sensor was developed through interdigital electrodes and presented the high-performance temperature sensing property, demonstrating it would be a good potential in variety of flexible inorganic semiconductor microdevices as well as tiny integrated devices.

1. Introduction

Molybdenum trioxide (MoO_3), as a typical transition-metal oxides, has recently gained increasing interests owing to its unique layered structure, rich chemistry associated with multiple valence states, high thermal and chemical stability [1–5]. It is an excellent candidate in a variety of applications, such as catalysts [4], gas sensors [6], lithium-ion batteries [7], field emission [8,9], electrochromic and photochromic devices [10,11]. In general, there are three kinds of polymorphs for MoO_3, namely, thermodynamically stable phase of orthorhombic α-MoO_3, two metastable phases of monoclinic β-MoO_3 with ReO_3-type structure and hexagonal *h*-MoO_3 [12]. Moreover, the unique functional performance of MoO_3 are closely associated with its crystal structure, morphology and dimension. Up to now, the nanostructures of MoO_3 with different morphology, including nanorods [6], nanoparticles [4,13], nanotubes [14], nanobelts [7,8,10,15], nanowires [9], nanofibers and nanoplatelets [16], had been fabricated by a variety of synthesis methods. Representatively, Chithambaraj et al. [13] and Hu et al. [14] had successfully synthesized MoO_3 nanoparticles and nanotubes by a hydrothermal method. Additionally, Li et al. [8] and Cai et al. [12] demonstrated the α-MoO_3 nanobelts by using infrared irradiation heating method and flame synthesis technique. Furthermore, Zhou et al. [9] had reported the preparation of the α-MoO_3 nanowires by using a thermal evaporation method under vacuum conditions on Si substrates. Also, Li et al. [8] prepared MoO_3 nanobelts on a Si wafer via directly oxidizing a Mo foil, at ambient atmosphere, by infrared irradiation heating. Ding et al. [17] synthesized MoO_3 nanobelts and microballs by thermal oxidization of Mo wires with the temperature range from 500 to 1200 °C in an ambient atmosphere.

However, these synthesis methods have their limitations. For examples, the hydrothermal method needs the relatively complex synthesis processes, the flame synthesis method need inflammable and explosive gas ($CH_4 + H_2$) as fuels, and the thermal evaporation method require the use of catalysts and substrates or vacuum condition. In recent years, there is no report about in-situ synthesis of large area flexible aligned MoO_3 microsheets arrays (MMAs) via directly oxidizing the Mo foils at ambient atmosphere with the method of thermal oxidization. Furthermore, with the rapid development of portable and wearable electronics, this kind of flexible inorganic semiconductor devices, owing to their remarkable advantages such as light weight, mechanical flexibility, portability, and design freedom [18,19], will be applied in displays [20], energy storage devices [21,22], gas sensor devices [18,19,23,24], and ultraviolet detectors [25,26].

In present work, we report a facile and effective in-situ preparation method of flexible MMAs by directly oxidizing molybdenum

* Corresponding author.
E-mail address: wqyang@swjtu.edu.cn (W. Yang).

http://dx.doi.org/10.1016/j.jallcom.2016.11.365
0925-8388/

(Mo) metal in ambient condition. In comparison with the other synthesis methods, the method of thermal oxidation is much simple, economical, environment friendly and convenient for large quantity production. Moreover, based on it, we developed a simple and high-performance temperature sensor through interdigital electrodes, evidently presenting the potential applications for the flexible inorganic semiconductor microdevices as well as portable tiny integrated devices.

2. Experiments

The in-situ fabrication of aligned MMAs was based on thermal oxidization of Mo metal in an ambient condition with different temperature. Fig. 1a sketches the aligned MMAs on the Mo foil. In this experiment, a Mo foil (12 × 8 × 0.1 mm, in Fig. 1b) was heated in ambient atmosphere from room temperature to 400 °C, 500 °C, and 600 °C at a heating rate of 5 °C min^{-1} and then kept at the corresponding temperature for 90 min. The large area aligned MMAs (in Fig. 1c) product was obtained after the furnace was naturally cooled to room temperature. Uniquely, the Mo foil was placed in the alumina boat (60 × 30 × 15 mm), which completely covered with the same size of alumina boat for limiting oxygen concentration. From Fig. 1, it can be clearly found that a gray layer on the Mo foil in Fig. 1c, indicating that the surface of the Mo foil had already been oxidized.

The morphologies of the samples were examined by SEM (FEI-Quanta 200, Philips, Netherlands). The crystal structure phases of the as-obtained products were characterized by X-ray diffraction (XRD, X'PertPro, Philips, Netherlands). The main parameters of XRD are as follows: Cu K_α radiation was used, the X-ray generator was operated at 40 kV and 40 mA. Data sets were collected within the range of 10–70° with the scanning speed of 0.02°/s at room temperature.

Copper, as the interdigital electrodes of MMAs thin films, was deposited on the substrate by Physical Vapor Deposition (PVD). Firstly, put the copper and MMAs (1.2 × 1.5 cm) into the vacuum chamber, and the distance between the target and the substrate was 15 cm. Subsequently, the vacuum chamber was pumped down to a pressure of 8 × 10^{-4} Pa. The electrodes evaporated from the copper target had been deposited on the MMAs for 15 min. Finally, the samples were carefully taken out. The sketch and photograph (upright) of as-prepared temperature sensor are shown in Fig. 2.

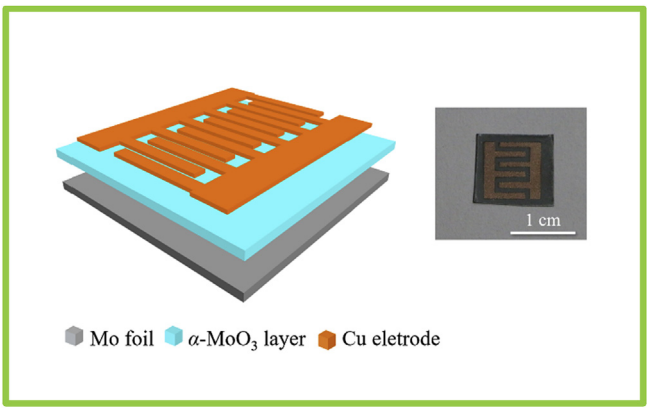

Fig. 2. The schematic structure of the MMAs temperature-sensor. The photograph of temperature sensor is upright.

3. Results and discussion

Fig. 3 shows the X-ray diffraction spectra of MMAs oxidized at different temperatures. All of the MoO_3 thin films can be indexed to an orthorhombic α-MoO_3 phase (JCPDS card No. 05-0508) [5] with the lattice constants of a = 3.962 Å, b = 13.858 Å, c = 3.697 Å and *Pbnm* space group, and no impurities peaks from any other impurities were detected by XRD, which indicting the high purity of the products. Three prominent peaks of XRD patterns appear at 23.339°, 45.759°, 46.319°, corresponding to the (110), (200) and (210) planes, respectively. Moreover, with the increasing oxidization temperature of from 400 °C to 600 °C, the XRD pattern presents the fine controllability. The intensity in the (110) plane becomes weaker, but the intensity in the (200) plane becomes stronger, evidently demonstrating that the preferential orientation of the (110) direction of MoO_3 crystallites formed at the lower temperatures, and the preferential orientation of the (200) direction of MoO_3 crystallites formed at the higher temperatures. When the temperature increased to 600 °C, the XRD pattern exhibits nearly the single (200) diffraction peak. For oxidization-growth α-

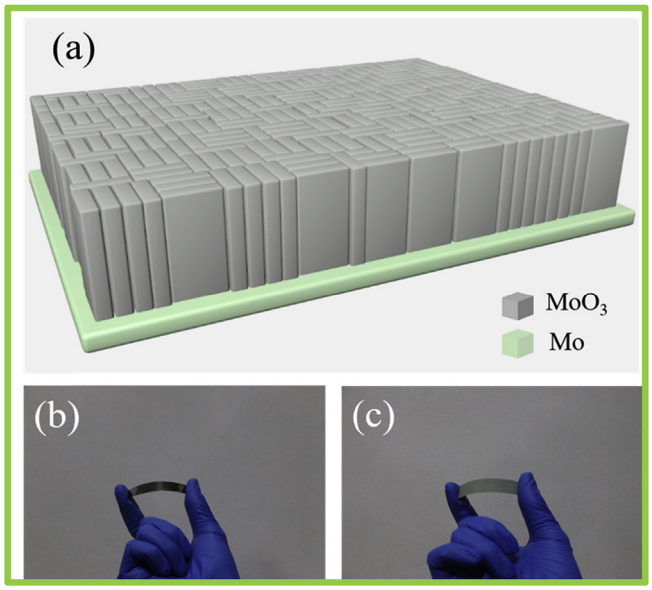

Fig. 1. The schematic structure (a) of flexible aligned α-MoO_3 microsheets arrays and the before (b) and after (c) oxidization of the Mo foil.

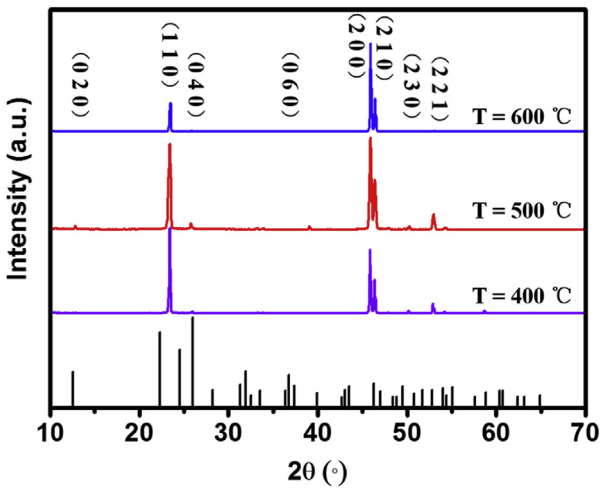

Fig. 3. XRD patterns of the samples obtained by heating at different temperatures for 90 min.

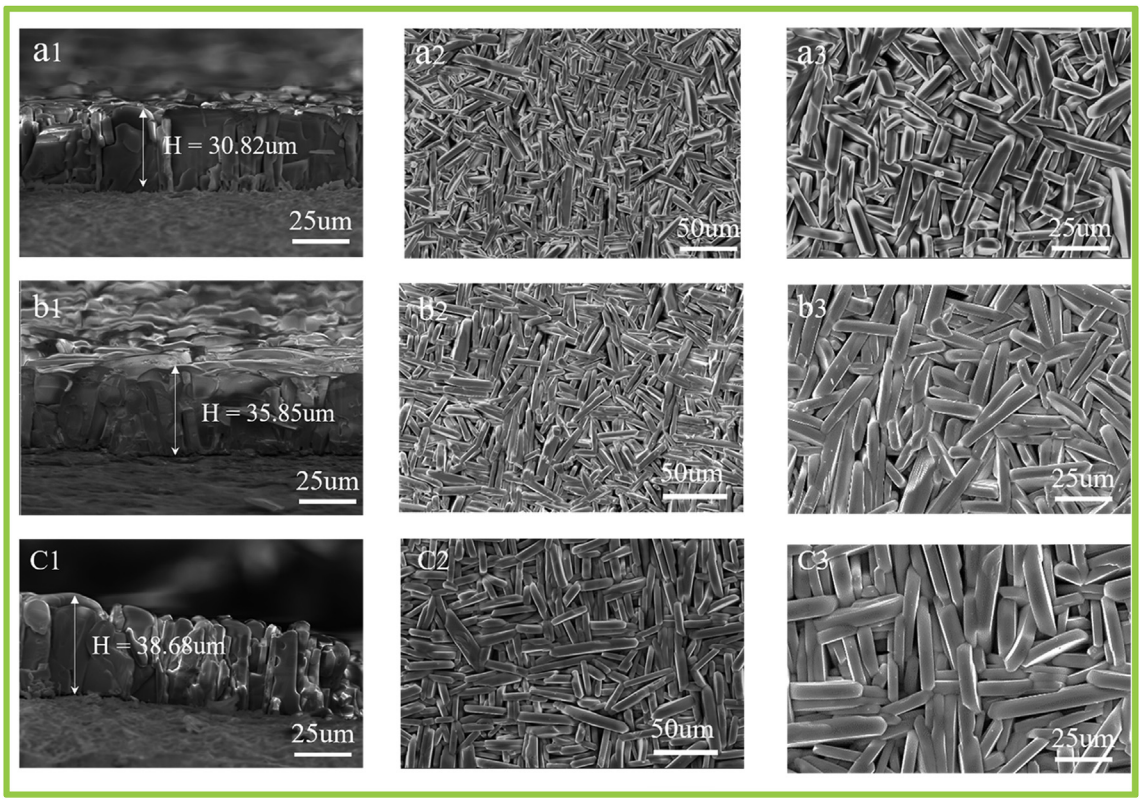

Fig. 4. The cross section SEM images (a1, b2, c3), low (a2, b2, c2) and high (a3, b3, c3) magnification SEM images of α-MoO_3 thin films at the oxidation temperature of from 400 °C to 600 °C.

MoO_3 crystallites, the XRD pattern is quite different from the others which shows nearly the (0*k*0) peaks (with even *k* values).

The morphologies and the sizes of MMAs were illuminated by SEM observations. Fig. 4 shows the surface and cross-sectional SEM images of α-MoO_3 films prepared with different oxidization temperature. From Fig. 4, we clearly found that, no matter which temperature was used, the as-obtained α-MoO_3 films have the structures of aligned microsheets arrays. From the cross-sectional SEM images (Fig. 4a1, b1, and c1), we can see that the height of MMAs, which obtained with the range of oxidization temperature from 400 °C to 600 °C, are about 30.82 μm, 35.85 μm, 38.68 μm, respectively. It is obviously ascribed that the height of the MMAs and the speed of growth increases with the increasing oxidization temperature. In addition, in the low (Fig. 4a2, b2, and c2) and high (Fig. 4a3, b3, and c3) magnification SEM images of α-MoO_3 films, we can easily find that the surface of α-MoO_3 thin films compose of rectangle geometries, whether in the low or high magnification, the size of rectangle obviously increases with the increasing temperature. More importantly, we can apply such a simple direct oxidizing method to controllably prepare large area flexible MMAs films, which can be expanded for the potential flexible inorganic semiconductor or even miniaturized integrated devices.

Based on this MMAs, we developed the simple temperature sensor by sputtering the interdigital copper electrode. Fig. 2 presents the sketch and photograph (upright) of as-prepared temperature sensor. Furthermore, we investigated the temperature sensing properties of the above sensor in detail. As shown in Fig. 5, these sensors present the high-performance sensitivity for environmental temperatures. Here, the sensitivity is defined as $S = R_e/R_r$ (R_e and R_r are the resistance for sensors at the environmental

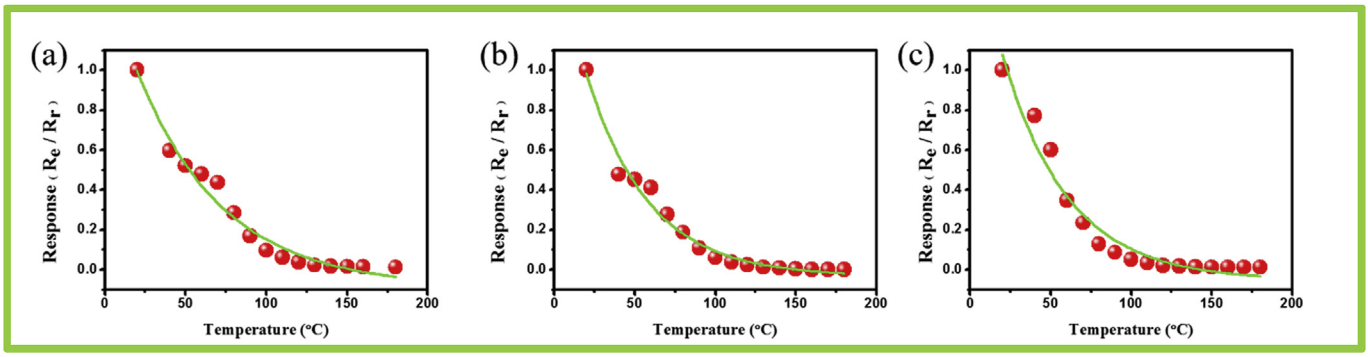

Fig. 5. The temperature-sensing properties of MMAs at various oxidization temperatures of 400 °C (a), 500 °C (b) and 600 °C (c) for environmental temperatures.

temperature and room temperature, respectively). Obviously, the temperature sensor based on MMAs at oxidization temperature of 600 °C show the best temperature sensing performance, which may be ascribed to the best crystallinity. Due to the limited experimental conditions, it is a pity that we could not develop the more excellent quality functional devices based on the as-grown MMAs. However, this kind of facile, environmentally friendly, in-situ growth, flexible and aligned MMAs obviously demonstrates the wider applications for flexible inorganic semiconductor microdevices as well as portable tiny integrated devices.

4. Conclusion

In summary, we applied a facile, environmentally friendly, in-situ growth and economic thermal oxidization method successfully to grow the large area, flexible and aligned semiconductor MMAs on Mo foil. The aligned MMAs arrays presents a preferential (100) orientation of the crystallites and the excellent flexibility. Moreover, we developed a simple temperature sensor with high-performance temperature sensing properties, evidently demonstrating this MMAs should be a good potential in variety of flexible inorganic microdevices as well as tiny integrated devices.

Acknowledgements

This work was supported by the scientific and technological projects for Distinguished Young Scholars of Sichuan Province (grant numbers 2015JQ0013), the Fundamental Research Funds for the Central Universities of China (grant numbers A0920502051408).

References

[1] X. Wen, W. Yang, Y. Ding, S. Niu, Z.L. Wang, Piezoresistive effect in MoO_3 nanobelts and its application in strain-enhanced oxygen sensors, Nano Res. 7 (2014) 180–189.
[2] L.X. Song, M. Wang, S.Z. Pan, J. Yang, J. Chen, J. Yang, Molybdenum oxide nanoparticles: preparation, characterization, and application in heterogeneous catalysis, J. Mater. Chem. 21 (2011) 7982–7989.
[3] H. Zhang, G. Yao, L. Wang, Y. Su, W. Yang, Y. Lin, 3D Pt/MoO_3 nanocatalysts fabricated for effective electrocatalytic oxidation of alcohol, Appl. Surf. Sci. 356 (2015) 294–300.
[4] W. Yang, Z. Wei, M. Gao, Y. Chen, J. Xu, C. Chen, Y. Lin, Fabrication and field emission properties of needle-shaped MoO_3 nanobelts, J. Alloys Compd. 576 (2013) 332–335.
[5] W. Yang, Z. Wei, X. Zhu, D. Yang, Strong influence of substrate temperature on the growth of nanocrystalline MoO_3 thin films, Phys. Lett. A 373 (2009) 3965–3968.
[6] E. Comini, L. Yubao, Y. Brando, G. Sberveglieri, As sensing properties of MoO_3 nanorods to CO and CH_3OH, Chem. Phys. Lett. 407 (2005) 368–371.
[7] R. Nadimicherla, Y.L. Liu, K.Q. Chen, W. Chen, Electrochemical performance of new α-MoO_3 nanobelt cathode materials for rechargeable Li-ion batteries, Solid State Sci. 34 (2014) 43–48.
[8] Y.B. Li, Y. Bando, D. Golberg, K. Kurashima, Field emission from MoO_3 nanobelts, Appl. Phys. Lett. 81 (2002) 5048–5050.
[9] J. Zhou, S.Z. Deng, N.S. Xu, J. Chen, J.C. She, Synthesis and field-emission properties of aligned MoO_3 nanowires, Appl. Phys. Lett. 83 (2003) 2653–2655.
[10] B. Gao, Q.F. Hui, J.Z. Xiao, J. Phys, Hydrothermal synthesis of single crystal MoO_3 nanobelts and their electrochemical properties as cathode electrode materials for rechargeable lithium batteries, Chem. Solids 73 (2012) 423–429.
[11] P. Jittiarporn, L. Sikong, K. Kooptarnond, W. Taweepreda, Effects of precipitation temperature on the photochromic properties of h-MoO_3, Ceram. Inter. 40 (2014) 13487–13495.
[12] P. Badica, Preparation through the vapor transport and growth mechanism of the first-order hierarchical structures of MoO_3 belts on sillimanite fibers, Cryst. Growth Des. 7 (4) (2007) 794–801.
[13] A. Chithambararaj, A.C. Bose, Hydrothermal synthesis of hexagonal and orthorhombic MoO_3 nanoparticles, J. Alloys Compd. 509 (2011) 8105–8110.
[14] S. Hu, X. Wang, Single-walled MoO_3 nanotubes, J. Am. Chem. Soc. 130 (2008) 8126–8127.
[15] L. Cai, P.M. Rao, X. Zheng, Morphology-controlled flame synthesis of single, branched, and flower-like α-MoO3 nanobelt arrays, Nano Lett. 11 (2011) 872–877.
[16] S.Z. Li, C.L. Shao, Y.C. Liu, S.S. Tang, R.X. Mu, Nanofibers and nanoplatelets of MoO_3 via an electrospinning technique, J. Phys. Chem. Solids 67 (2006) 1869–1872.
[17] Q.P. Ding, H.B. Huang, J.H. Duan, J.F. Gong, S.G. Yang, X.N. Zhao, Y.W. Du, Molybdenum trioxide nanostructures prepared by thermal oxidization of molybdenum, J. Cryst. Growth 294 (2006) 304–308.
[18] M. Asad, M.H. Sheikhi, M. Pourfath, M. Moradi, High sensitive and selective flexible H2S gas sensors based on Cu nanoparticle decorated SWCNTs, Sens. Actuat. B 210 (2015) 1–8.
[19] B. Hu, W. Chen, J. Zhou, High performance flexible sensor based on inorganic nanomaterials, Sens. Actuat. B 176 (2013) 522–533.
[20] T. Sekitani, T. Yokota, U. Zschieschang, H. Klauk, S. Bauer, K. Takeuchi, M. Takamiya, T. Sakurai, T. Someya, Organic nonvolatile memory transistors for flexible sensor arrays, Science 326 (2009) 1516–1519.
[21] H. Zhang, H. Su, L. Zhang, B. Zhang, F. Chun, X. Chu, W. He, W. Yang, Flexible supercapacitors with high areal capacitance based on hierarchical carbon tubular nanostructures, J. Power Sources 331 (2016) 332–339.
[22] Y. He, W. Chen, C. Gao, J. Zhou, X. Li, E. Xie, An overview of carbon materials for flexible electrochemical capacitors, Nanoscale 5 (2013) 8799–8820.
[23] K. Cattanach, R.D. Kulkarni, M. Kozlov, S.K. Manohar, Flexible carbon nanotube sensors for nerve agent simulants, Nanotechnology 17 (2006) 4123–4128.
[24] L. Zhang, Z. Liu, L. Jin, B. Zhang, H. Zhang, M. Zhu, W. Yang, Self-assembly gridding α-MoO_3 nanobelts for highly toxic H2S gas sensors, Sens. Actuat. B 237 (2016) 350–357.
[25] Y.R. Tao, J.Q. Chen, J.J. Wu, Y. Wu, X.C. Wu, Flexible ultraviolet–visible photodetector based on HfS_3 nanobelt film, J. Alloys Compd. 658 (2016) 6–11.
[26] D.I. Son, H.Y. Yang, T.W. Kim, W.I. Park, Transparent and flexible ultraviolet photodetectors based on colloidal ZnO quantum dot/graphene nanocomposites formed on poly (ethylene terephthalate) substrates, Compos. Part B Eng. 69 (2015) 154–158.